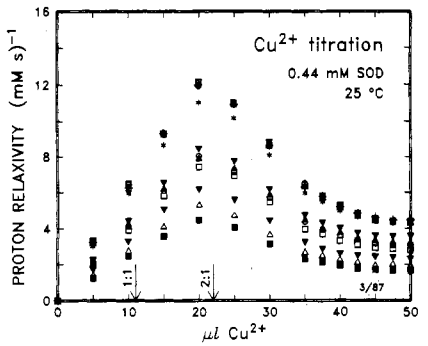

Figure 3. Titration of 20 mM Cu^{2+} into (dimeric) apoSOD. Data at all the fields of Figure 2 are shown, from 0.01 MHz at the top to 50 MHz at the bottom. A clear break in the rates is seen when all the copper sites are filled, indicating strong binding at the Cu^{2+} site; the subsequent monotonic, but nonlinear, decrease indicates weaker binding of Cu^{2+} to the zinc sites as well as the nature of the Cu^{2+}–Cu^{2+} interaction (see text).

electronic dipolar interactions. The underlying physical principle is rather straightforward and can be described rather directly for coupled $S = {}^1/_2$ systems: In the absence of an exchange interaction between the Cu^{2+} ions, the quantization of both the nuclei and the electrons is, to first order, along the direction of the applied field. Thus, the nuclear and electronic moments are always either parallel or antiparallel to each other, and the energy levels and transitions are determined accordingly. When two Cu^{2+} spins become tightly coupled, the quantization of each Cu^{2+} spin is along the exchange field of the other and only the net spin (here, $S = 1$) is quantized along the external field. The electron spin of a single Cu^{2+} ion is then no longer a good quantum number, and one must look at its orientation in space for each state of the $S = 0$ and $S = 1$ manifolds to obtain the nuclear–electronic interaction. Thus, two Cu^{2+} spins combine to give a triplet with $S = 1$ and total $M = 1, 0, -1$ and a singlet with $S = 0$ and $M = 0$. For the $M = 0$ levels, i.e., two of the four levels, there is no component of electronic moment along the field direction (along which the nuclei are quantized) and, therefore, no nuclear interaction (either hyperfine[18] or dipolar[8]). Thus, only half the levels give a nonzero interaction with the nuclei for coupled ions with $S = 1$, and the source of the factor ${}^1/_2$ is immediate. For coupled ions with $S > {}^1/_2$, the appropriate factor is not so obvious and one must resort to the formalism of Bertini et al.,[8] who have tabulated the factor for a range of spin values, assuming that all levels are uniformly populated. Moreover, their formalism can readily be extended to the case when the spacings of the manifolds are comparable to kT.

Thus, it follows that for Cu_2Cu_2SOD, assuming that its ligand configuration is the same as that of Cu_2Zn_2SOD, theory predicts that the amplitude of the NMRD profile should be precisely half that of Cu_2Zn_2SOD when the exchangeable protons on one Cu^{2+} ion are too far from the other Cu^{2+} ion to be affected by its dipolar field. Since the theoretical treatment of the dipolar relaxation of a liganded proton also requires knowledge of the hyperfine coupling between the Cu^{2+} ion and its nucleus, we have used the value of the EPR hyperfine coupling found for the monomer since the decrease in hyperfine interaction due to pairing is incorporated implicitly in the above considerations. For Cu_2Cu_2SOD, we find the same r_{Cu-H} as for Cu_2Zn_2SOD and a slightly longer $\tau_S = 4.2 \times 10^{-9}$ s (cf. Table I). It appears, therefore, that the electronic relaxation time of the Cu^{2+} ion that binds water is not altered detectably when Cu^{2+} is brought into interaction with a nearby, second, Cu^{2+} ion. This important fact has not been uncovered by EPR spectroscopy.

Considering the normalized relaxation rates at selected fields as a function of copper content (Figure 3), we note that the relaxivities increase linearly up to 2:1 copper to dimeric protein ratio (giving no indication of a protein monomer–monomer interaction), then decrease linearly until about 3.5:1, and level off near a ratio of 4:1. The initial decrease is due to the abrupt onset of magnetically coupled pairs of adjacent Cu^{2+} ions once the copper sites are filled and Cu^{2+} ions begin to occupy the zinc sites, combined with the absence of any contribution to the relaxivity from the Cu^{2+} ions in the zinc sites. The titration shows clearly that binding of Cu^{2+} to the native copper sites is quantitative under the present experimental conditions, indicating very tight binding, whereas the subsequent binding to the zinc sites is weaker. An upper limit of 10^{-6} M for the affinity constant of Cu^{2+} for Cu_2E_2SOD can be estimated from the present data, consistent with previous findings under different conditions.[20,21]

Concluding Remarks

The apoSOD/Cu^{2+} system is particularly tractable for generating magnetically coupled Cu^{2+} pairs in a macromolecular environment, so as to allow refinement of the theoretical basis of electronic relaxation of coupled paramagnetic ions. It has the advantage that the first equivalent of Cu^{2+} binds to the copper site of SOD quantitatively, yielding a single species that can be interpreted unambiguously. In addition, Cu^{2+} enters the zinc site; no direct effect on the NMRD profile is expected since there is no inner-coordinated water there. Rather, the influence of the second Cu^{2+} is through alteration of the interaction between the Cu^{2+} ions in the copper site and the protons they relax. The theory corroborates that this is the dominant effect; in essence, the J splitting of the levels of the paired Cu^{2+} ions (large compared to the widths of the electronic levels, but small compared to kT), alters the quantization direction of the individual Cu^{2+} ions and makes half the levels ineffective in proton dipolar[8] and nuclear hyperfine[18] interactions, causing the relaxivity to decrease by half. By contrast, the electronic relaxation times are not significantly altered in the Cu^{2+} dimer, despite the strong magnetic coupling; i.e., the mechanism that couples the magnetic energy of the paramagnetic ions to the protein is essentially unaltered by the pairing of the two Cu^{2+} ions and the concomitant rapid exchange of electronic spin within the Cu^{2+} dimer. This is a new result and is particularly relevant for understanding NMR, NMRD, EPR, and ENDOR experiments on this and related systems of paired, magnetically coupled, paramagnetic ions.

Registry No. Cu^{2+}, 15158-11-9.

(20) Hirose, J.; Iwatzuka, K.; Kidani, Y. *Biochem. Biophys. Res. Commun.* **1981**, *98*, 58.
(21) (a) Rigo, A.; Viglino, P.; Calabrese, L.; Cocco, D.; Rotilio, G. *Biochem. J.* **1977**, *161*, 27. (b) Rigo, A.; Terenzi, M.; Viglino, P.; Calabrese, L.; Cocco, D.; Rotilio, G. *Biochem. J.* **1977**, *161*, 31.

Contribution from the Anorganisch Chemisch Laboratorium, University of Amsterdam, Nieuwe Achtergracht 166, 1018 WV Amsterdam, The Netherlands, and Department of Chemistry, York University, North York, Ontario, Canada M3J 1P3

Semiquinone–Quinone Redox Species Involving Bis(bipyridine)ruthenium(II): Resonance Raman Spectra

D. J. Stufkens,*[1a] Th. L. Snoeck,[1a] and A. B. P. Lever*[1b]

Received July 16, 1987

Haga, Dodsworth, and Lever[2] recently reported the UV/visible, IR, and ESR spectra together with the electrochemical data of a series of complexes belonging to the redox chain RuN_4(cat), $[RuN_4(sq)]^+$, and $[RuN_4(q)]^{2+}$ where the N_4 units were bis(bipyridine) or tetrakis(pyridine) and the dioxolene ligands were catechols (cat) and their one- and two-electron oxidation products, semiquinones (sq) and quinones (q), respectively. All data confirmed that these complexes contain ruthenium(II). The electronic spectra were reported and assigned by correlation with the elec-

(1) (a) University of Amsterdam. (b) York University.
(2) Haga, M. A.; Dodsworth, E. S.; Lever, A. B. P. *Inorg. Chem.* **1986**, *25*, 447.

0020-1669/88/1327-0953$01.50/0

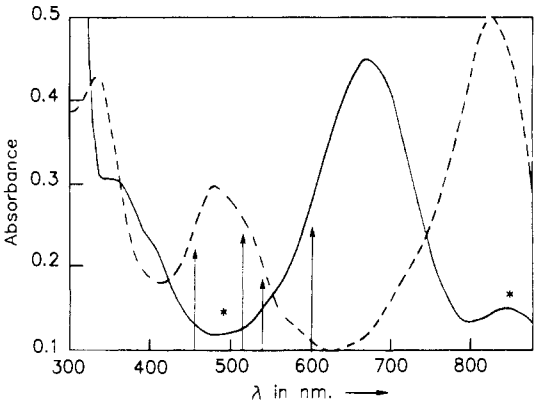

Figure 1. Electronic spectra of $[Ru^{II}(bpy)_2(DTBSq)](PF_6)$ (**1**-PF_6, ---) and $[Ru^{II}(bpy)_2(Q)](ClO_4)_2$ (**2**, —) in 1,2-dichloroethane (the former from ref 2). The arrows indicate the laser frequencies used to excite the rR spectra. The spectrum of **2** shows a small amount of unoxidized semiquinone species marked by asterisks.

trochemical potentials and their dependence upon change of catechol substituent. The semiquinone members of this series exhibited very low energy near-infrared absorption, and extensive mixing of this low excited state with the ground state was inferred.

Resonance Raman (rR) spectroscopy is a valuable technique for the assignment of absorption bands and, more importantly, for learning more of the nature of the electronic state concerned.[3,4] In this article we report the rR spectra of two complexes of the above series, viz. $[Ru(bpy)_2(DTBSq)]^+$ (**1**) and $[Ru(bpy)_2(Q)]^{2+}$

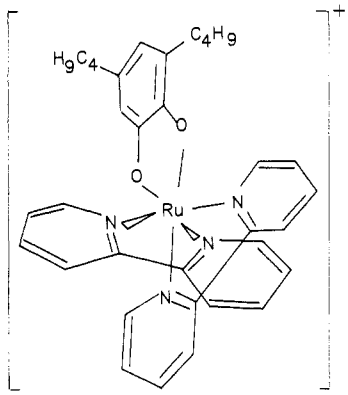

1

(**2**) (bpy = 2,2′-bipyridine, DTBSq = 3,5-di-*tert*-butyl-*o*-semiquinonate(1−), Q = *o*-quinone(0)). Unfortunately, the rR spectra of the reduced species $Ru(bpy)_2(DTBCat)$ could not be recorded because of the instability of the complex to oxidation.

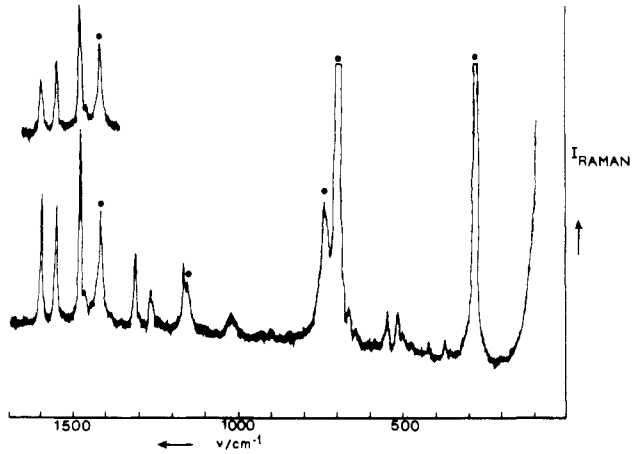

Figure 2. Resonance Raman spectrum of $[Ru^{II}(bpy)_2(DTBSq)](PF_6)$ (**1**-PF_6) in dichloromethane (excitation at 514.5 nm). Insert: Excitation at 540 nm. Bands indicated with a ● are solvent bands. Enhanced bands are observed at 354, 374, 519, 551, 667, 1024, 1167, 1268, 1315, 1485, 1556, and 1604 cm^{-1}.

Experimental Section

Complexes **1** and **2** were prepared according to literature methods.[2] The rR spectra were recorded in a spinning cell by using a Jobin Yvon HG2S Ramanor. The samples were excited by an SP Model 171 argon ion laser and a tunable CR490 dye laser with Rhodamine 6G as dye. Laser power was 50–100 mW, and spectral slit width was 10 cm^{-1}. Controlled-potential oxidation was carried out in dichloromethane or 1,2-dichloroethane with tetrabutylammonium perchlorate as supporting electrolyte.

Results and Discussion

$[Ru^{II}(bpy)_2(DTBSq)]^+$ (1). The absorption spectrum of **1** shows three visible-region bands at about 350, 500, and 850 nm, with evidence of shoulders (Figure 1). The band at 500 nm occurs at an energy comparable to that of the MLCT band of the $[Ru^{II}(bpy)_3]^{2+}$ ion[4a] **3** and is absent from the spectrum for the tetrakis(pyridine) species. It was accordingly assigned[2] to Ru(II) → (bpy)π_1* transitions. In agreement with this assignment the charge-transfer transitions to the (bpy)π_2* orbitals are observed at 350 nm. Normally, transitions to π_1* and π_2* differ in energy by 7000–9000 cm^{-1}.[2,5] The band at about 850 nm and the 600-nm shoulder of the 500-nm band for **1** are not present in the absorption spectrum of **3**, which suggests they belong to transitions involving the DTBSq ligand. They are assigned[2] to Ru(II) → DTBSq and DTBSq → (bpy)π_1* (or perhaps to internal DTBSq n → π_1*) transitions, respectively.

rR spectra have been measured to confirm these assignments and to seek further information concerning the electronic nature of these species. Unfortunately, the 350- and 850-nm bands are outside the wavelength region of our laser lines, so that only the properties of the 500-nm band and its shoulder could be studied. The rR spectra have been measured with exciting laser lines of 458, 514, 540, and 600 nm, and a representative spectrum is shown in Figure 2.

The spectra show resonance enhancement for bands at 1604, 1556, 1485, 1315, 1268, 1167, 1024, and 667 cm^{-1}, all belonging to vibrations of the complexed bpy ligand.[4] The same bands are observed in the rR spectra of **3** and $Ru^{II}(bpy)_2Cl_2$[4b] and are typical of those expected for coupling to a Ru(II) → bpy metal to ligand charge-transfer transition (MLCT). A metal–nitrogen stretching mode is observed at 374 cm^{-1}, and with 514-nm excitation, there is a second, very weak band observed at 354 cm^{-1}.

There is a gradual change of the relative intensities of the bpy modes at 1604, 1556, and 1485 cm^{-1} when the wavelength of the exciting laser is varied from 458 to 600 nm. Upon 458-nm excitation, the 1604-cm^{-1} band is the strongest, whereas this band is the weakest in the spectra excited at 540 nm and at longer wavelengths (see insert of Figure 2).

(3) (a) Clark, R. J. H.; Stewart, B. *Struct. Bonding (Berlin)* **1979**, *36*, 1. (b) Clark, R. J. H.; Dines, T. J. *Angew. Chem.* **1986**, *25*, 131. (c) Balk, R. W.; Snoeck, Th. L.; Stufkens, D. J.; Oskam, A. *Inorg. Chem.* **1980**, *19*, 3015. (d) Servaas, P. C.; van Dijk, H. K.; Snoeck, Th. L.; Stufkens, D. J.; Oskam, A. *Inorg. Chem.* **1985**, *24*, 4494.

(4) (a) Mabrouk, P. A.; Wrighton, M. S. *Inorg. Chem.* **1986**, *25*, 526. (b) Basu, A.; Gafney, H. D.; Strekas, Th. C. *Inorg. Chem.* **1982**, *21*, 2231. (c) Caspar, J. V.; Westmoreland, T. D.; Allen, G. H.; Bradley, P. G.; Meyer, T. J. *J. Am. Chem. Soc.* **1984**, *106*, 3492. (d) Strukl, J. S.; Walter, J. L. *Spectrochim. Acta, Part A* **1971**, *27A*, 209. (e) Poizat, O.; Sourisseau, C. *J. Phys. Chem.* **1984**, *88*, 3007. (f) Braunstein, C. H.; Baker, A. D.; Strekas, T. C.; Gafney, H. D. *Inorg. Chem.* **1984**, *23*, 857. (g) Fuchs, Y.; Lofters, S.; Dieter, T.; Shi, W.; Morgan, R.; Strekas, T. C.; Gafney, H. D.; Baker, A. D. *J. Am. Chem. Soc.* **1987**, *109*, 2691. (h) Caswell, D. S.; Spiro, T. G. *Inorg. Chem.* **1987**, *26*, 18. (i) Tait, C. D.; Donohoe, R. J.; DeArmond, M. K.; Wertz, D. W. *Inorg. Chem.* **1987**, *26*, 2754. (j) Chung, Y. C.; Leventis, N.; Wagner, P. J.; Leroi, G. E. *J. Am. Chem. Soc.* **1985**, *107*, 1416. (k) Angel, S. M.; DeArmond, M. K.; Donohoe, R. J.; Wertz, D. W. *J. Phys. Chem.* **1985**, *89*, 282. (l) Angel, S. M.; DeArmond, M. K.; Donohoe, R. J.; Hanck, K. W.; Wertz, D. W. *J. Am. Chem. Soc.* **1984**, *106*, 3688. (m) Balk, R. W.; Stufkens, D. J.; Crutchley, R. J.; Lever, A. B. P. *Inorg. Chim. Acta* **1982**, *64*, L49. (n) Donohoe, R. J.; Tait, C. D.; DeArmond, M. K.; Wertz, D. W. *Spectrochim. Acta, Part A* **1986**, *42A*, 233.

(5) van Dijk, H. K.; Stufkens, D. J.; Oskam, A., manuscript in preparation.

For the explanation of this effect we rely on a recent rR study of the complex $Fe_2(CO)_6(bpy)(P(n\text{-}Bu)_3)$,[5] which has its Fe(0) → (bpy)π_1* and Fe(0) → (bpy)π_2* MLCT transitions at much lower energies (maxima at 420 and 645 nm, respectively, in 2-methyltetrahydrofuran) than the complex ion under study. In the rR spectrum of the Fe complex, excited in preresonance with the transitions to (bpy)π_1* (600-nm excitation), the intensity of the 1600-cm^{-1} bpy band is only one-third of that of the 1485-cm^{-1} band. Both bpy bands, however, have nearly the same intensities in the rR spectrum excited at 458 nm, in preresonance with the transitions to (bpy)π_2*. Accordingly, the increase of relative intensity of the 1604-cm^{-1} band of **1** upon excitation at higher energy is ascribed to a preresonance Raman effect of the Ru(II) → (bpy)π_2* transitions at 350 nm. Further support for this explanation is supplied by the rR intensity of the 1604-cm^{-1} band which increases with respect to the close-lying solvent band upon going from 488- to 458-nm excitation, although all other vibrations decrease in intensity. These rR results agree with the assignment of the 500-nm band by Lever and co-workers[2] to Ru(II) → (bpy)π_1* transitions.

During these transitions the metal–nitrogen bonds are hardly affected, since the corresponding metal–nitrogen modes at 374 and 354 cm^{-1} only show very weak rR effects. In one crucial respect these rR spectra differ from those of **3**, since in **1** two extra (weak) bands are observed at 551 and 519 cm^{-1}, respectively. The intensities of these transitions increase with respect to those of the 374- and 354-cm^{-1} bands upon excitation with longer wavelength light. In agreement with the assignments for other complexes of chelating oxygen donor ligands,[6] these new bands are assigned to metal–oxygen stretching modes, coupled to μ(CC) and ring deformation modes of the DTBSq ligand.

The appearance of these bands is probably caused by coupling of these modes to the Ru(II) → (bpy)π_1* transitions, which will certainly influence the metal–oxygen bonds. Their increase in intensity with respect to the metal–nitrogen stretching modes upon going to longer wavelength excitation is then the result of a stronger interaction between the specific Ru d orbital involved in the transition at 540 nm (presumably Ru b_1; vide infra) and the DTBSq b_1 orbital. Alternatively, these rR effects might result from coupling of the metal–oxygen stretching modes to the weaker DTBSq → (bpy)π_1* (or DTBSq n → π*) transition[2] at about 600 nm. This resonance assignment is, however, rather unlikely in view of the weakness of this shoulder and of the observation of these bands already upon 488-nm excitation.

$[Ru^{II}(bpy)_2(Q)]^{2+}$ (2). Since better rR spectra could be obtained for the complex of the unsubstituted quinone ligand than for the corresponding DTBQ compound, the results for $[Ru(bpy)_2(Q)]^{2+}$ will be described here. The *tert*-butyl substituents appeared to have no significant influence on the absorption and rR spectra. The complex ion, which was prepared by controlled-potential oxidation[2] of a solution of the Sq complex (with tetrabutylammonium perchlorate) in $C_2H_4Cl_2$, was not isolated, but its absorption and rR spectra were measured from the solution directly after the oxidation was completed. The absorption spectrum (Figure 1) shows two bands at about 400 and 670 nm, which have been assigned[2] to Ru(II) → (bpy)π_1* and Ru(II) → (Q)π* ($3b_1$ in C_{2v} symmetry) MLCT transitions, respectively. rR spectra were measured with 458-nm excitation in preresonance with the 400-nm band and with 600-nm excitation in preresonance with the 670-nm band. The 458-nm-excited spectra only showed weak rR effects for the bpy bands at 1604, 1555, and 1487 cm^{-1}, in agreement with the assignment of the 400-nm band to Ru(II) → (bpy)π_1* transitions.

The 600-nm-excited spectra were completely different, the strongest rR effects now being observed for bands at 585, 560, and 516 cm^{-1} (Figure 3). Just as for the DTBSq complex, these bands will now have contributions from the metal–oxygen stretching modes, coupled to μ(CC) and ring deformation modes of the quinone ligand.[6] The high intensity of these rR modes

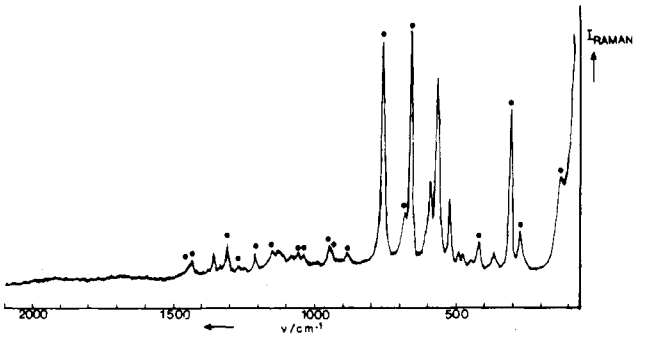

Figure 3. Resonance Raman spectrum of $[Ru^{II}(bpy)_2(Q)](ClO_4)_2$ (**2**-$(ClO_4)_2$) in 1,2-dichloroethane containing tetrabutylammonium perchlorate, (excitation at 600 nm). Bands indicated with a ● are solvent bands, and ◆ indicates a ClO_4^- band. Enhanced bands are observed at 360, 426, 473, 489, 516, 560, 585, 1072, 1125, 1351, 1487, 1555, and 1604 cm^{-1}.

implies that the metal–oxygen bonds are strongly affected by the electronic transition(s) involved in the 670-nm band. At the same time hardly any charge seems to be transferred to the quinone ligand during these transitions, since only very weak rR effects are observed for the stretching modes of the complexed quinone ligand at 1072, 1125, and 1351 cm^{-1}. These rR results agree with the assignment of the 670-nm band to Ru(II) → $3b_1$(Q) transitions. Comparing these latter rR results with those obtained upon excitation into the Ru(II) → (bpy)π_1* transitions, we observe remarkable differences in the relative intensities of the ligand and metal–ligand stretching modes, an effect that will now be discussed in more detail.

In **3** and its derivatives, the Ru(II) to bpy π-back-bonding is relatively small, and as a result the Ru(II) → (bpy)π_1* transitions have strong MLCT character. This electron transfer strongly affects the bond lengths of the bpy ligand (it is effectively bpy–), giving rise to the strong rR effects observed for the bpy stretching modes. The metal–bpy bonds will hardly be affected by this transition since loss of π-back-bonding will be compensated for by an increase of ionic interaction in the excited state. This latter result is in accordance with the conclusion of Rillema et al.[7] that $[Ru^{II}(bpy)_3]^{2+}$ and $[Ru^{II}(bpy)_3]^{2+*}$ have similar structures.

In contrast to the π_1* orbital of bpy, the low-lying $3b_1$(Q) orbital of the quinone ligand will be mixed with the filled d(b_1) orbital of Ru(II). As a result, the allowed electronic transition between these orbitals, which is mainly responsible for the high intensity of the 670-nm band, has hardly any MLCT character. Instead, it has become a metal–ligand bonding to antibonding transition (Ru(b_1) + $3b_1$(Q) → $3b_1$(Q)–Ru(b_1)). Because of this, the rR spectrum excited in preresonance with this transition only shows weak rR effects for the ligand-stretching modes. However, there should be very strong rR effects in the metal–quinone stretching modes in the 500–600-cm^{-1} region, as observed.

A similar change of MLCT character has been observed for a series of complexes of the α-diimines bpy, phen (phen = 1,10-phenanthroline), and R-DAB (R-DAB = R—N=CH—CH=NR; DAB = 1,4-diaza-1,3-butadiene), all possessing a low-lying π* orbital.[3d,8] Thus, the complexes $W(CO)_4(\alpha$-diimine) all show an intense MLCT band in the visible region. The main transition in this band is the W(0)(b_2) → (α-diimine)π*(b_2) transition. This π* orbital is lower in energy and has a better overlap with the filled metal d(b_2) orbital in the case of R-DAB than for bpy and phen.[9] This difference in metal–ligand interaction in $W(CO)_4$(R-DAB) on the one hand and $W(CO)_4$(bpy) and $W(CO)_4$(phen) on the other is strongly reflected in the rR spectra of these complexes. Both $W(CO)_4$(bpy) and $W(CO)_4$(phen) show

(6) Adams, D. M. *Metal-Ligand and Related Vibrations*; Arnold: London, 1967.

(7) Rillema, D. P.; Jones, D. S.; Levy, H. A. *J. Chem. Soc., Chem. Commun.* **1979**, 849.

(8) (a) Balk, R. W.; Stufkens, D. J.; Oskam, A. *J. Chem. Soc., Dalton Trans.* **1982**, 275. (b) van Dijk, H. K.; Servaas, P. C.; Stufkens, D. J.; Oskam, A. *Inorg. Chim. Acta* **1985**, *104*, 179.

(9) Reinhold, J.; Benedix, R.; Birner, P.; Hennig, H. *Inorg. Chim. Acta* **1979**, *33*, 209.

strong rR effects for the ligand stretching modes and only weak effects for the metal–ligand stretching modes upon excitation into the MLCT band. This result confirms the strong MLCT character of the metal to α-diimine transitions in these complexes, which is also evident from the large solvatochromism of these MLCT bands. The rR spectra of the $W(CO)_4$(R–DAB) complexes, on the other hand, do not show any rR effect for μ(s)(CN) of the R–DAB ligand but instead show strong rR effects for metal–ligand stretching and ligand deformation modes. This implies a lack of MLCT character for the transitions involved, which are now strongly metal–ligand bonding to antibonding. This lack of MLCT character is also evident from the absence of any solvent dependence of the position of the MLCT band.

In conclusion it can be said that the rR spectra of these Ru(II) complexes give valuable information not only about the correctness of previous assignments of absorption bands but also about the specific nature of the transitions involved.

Acknowledgment. We thank Dr. E. S. Dodsworth for useful discussion.

Contribution from the Centro di Studio sulla Stabilità e Reattività dei Composti di Coordinazione, CNR, Via Marzolo 1, 35131 Padova, Italy, Dipartimento di Chimica Inorganica, Metallorganica e Analitica, Università di Padova, Via Loredan 4, 35131 Padova, Italy, and Dipartimento di Chimica Organica, Centro di Studio sui Biopolimeri, CNR, Via Marzolo 1, 35131 Padova, Italy

Synthesis and Solvolytic Behavior of *cis*-(1,1′-Bis(diphenylphosphino)ferrocene)platinum(II) and -palladium(II) Complexes. X-ray Structure of Bis(μ-hydroxy)bis(1,1′-bis(diphenylphosphino)ferrocene)diplatinum(II) Tetrafluoroborate

Bruno Longato,*† Giuseppe Pilloni,‡ Giovanni Valle,§ and Benedetto Corain†

Received June 16, 1987

The fate of cis-platinum(II) drugs inside the cell cytoplasm as well as the mechanism of the selective lesion caused by them to DNA are still open questions.[1] Particularly relevant seems to be the hydrolytic cleavage of the Pt–Cl bonds, the consequent formation of aquo and/or hydroxo species, and their reactivity toward nucleotides.

We have recently reported[2] that (dppf)$PtCl_2$ (**1**-Pt) and $[(dppf)Pt(\mu\text{-}Cl)]_2^{2+}$ (**2**-Pt) (dppf) = 1,1′-bis(diphenylphosphino)ferrocene) are the precursors of the solvato complexes $[(dppf)PtClS]^+$ (**3**-Pt) and $[(dppf)PtS_2]^{2+}$ (**5**-Pt), which exhibit a remarkably high reactivity toward thymidines.

Preliminary in vitro tests on the cytostatic ability of complexes **1**-Pt and **2**-Pt have shown[3] that only the hydrolytically labile complex **2**-Pt, dissolved in DMSO, caused considerable growth inhibition of tumoral cells. Interestingly, the related complex $[(dppf)Pt(\mu\text{-}OH)]_2^{2+}$ (**4**-Pt) herein described turned out to be inactive and this observation prompted us to investigate the solution chemistry, i.e. solvolytic behavior, of complexes $[(dppf)M(\mu\text{-}Cl)]_2^{2+}$ (**2**, M = Pd, Pt) as well as of the related species $[(dppf)PtS_2]^{2+}$ (**5**-Pt, S = dimethylformamide) and $[(dppf)M(\mu\text{-}OH)]_2^{2+}$. We also report on the X-ray structure of **4**-Pt, which is, to the best of our knowledge, the second example of a hydroxo bis(phosphino) complex of platinum(II) for which the molecular structure has been determined by X-ray analysis.[4] Moreover, we herein describe some preliminary voltammetric tests concerning the reported complexes.

Experimental Section

General Procedures and Materials. All solvents were dried by standard procedures. ^1H and ^{31}P NMR spectra were recorded on a JEOL 90 Q spectrometer at 27 °C and were referenced to internal Me_4Si and external H_3PO_4 (85% w/w), respectively. IR spectra were recorded on a Perkin-Elmer Model 599 B spectrometer. UV–vis spectra were taken on a Perkin-Elmer LAMBDA 5 spectrometer. The apparatus used for voltammetry consisted of an Amel Model 551 potentiostat modulated by an Amel Model 566 function generator, while the recording device was a Hewlett-Packard 7040 A X-Y recorder. All experiments were performed at 25 °C in deoxygenated 1,2-dichloroethane (DCE) with 0.2 M tetrabutylammonium perchlorate (TBAP) as supporting electrolyte, with use of a conventional three-electrode liquid-jacketed cell. The working electrode was a planar Pt microelectrode (ca. 0.3 mm^2), surrounded by a Pt-spiral counter electrode. A silver/0.1 M silver perchlorate electrode in acetonitrile, separated from the working solution by a fine glass frit, was used as the reference electrode. All potentials are referred to the ferrocenium/ferrocene couple. 1,1′-Bis(diphenylphosphino)ferrocene (dppf) was from Strem Chemicals and was used as received, and (dppf)$PtCl_2$ was prepared as reported elsewhere.[14]

$[(dppf)M(\mu\text{-}Cl)]_2(BF_4)_2$ (2: M = Pt, 2-Pt; M = Pd, 2-Pd). A solution of $AgBF_4$ (0.119 g, 0.609 mmol) in acetone (10 mL) was added dropwise to a suspension of (dppf)$PtCl_2$ (0.500 g, 0.609 mmol) in acetone (30 mL). After it was stirred for 30 min, the reaction mixture was filtered and the filtrate was vacuum-evaporated to 5 mL. Addition of Et_2O afforded a burgundy red crystalline precipitate (0.424 g) in 80% yield. **2-Pd** was similarly obtained as a green product in 90% yield. IR (Nujol): 295 and 290 cm^{-1} (ν_{Pd-Cl}); 305 and 295 cm^{-1} (ν_{Pt-Cl}). ^{31}P NMR (CD_2Cl_2, 90 MHz): **2**-Pt, δ 18.30 (s, flanked by ^{195}Pt satellites, J = 3987 Hz); **2**-Pd, δ 46.5 (s). Anal. Calcd for $C_{34}H_{28}BClF_4FeP_2Pd$: C, 52.15; H, 3.60; Cl, 4.53. Found: C, 52.30; H, 3.60; Cl, 4.75. Calcd for $C_{34}H_{28}BClF_4FeP_2Pt$: C, 46.84; H, 3.24; Cl, 4.07. Found: C, 46.10; H, 3.23; Cl, 3.82.

$[(dppf)M(\mu\text{-}OH)]_2(BF_4)_2 \cdot 2CH_2Cl_2$ (4: M = Pt, 4-Pt;[5] M = Pd, 4-Pd). A solution of $AgBF_4$ (0.238 g, 1.218 mmol) in CH_3OH (5 mL) was added to a suspension of **1**-Pt (0.50 g, 0.609 mmol) in 25 mL of CH_3OH (reagent grade, 0.1% water content). The reaction mixture was stirred for 12 h in the open atmosphere and the solvent removed under vacuum. The residue was extracted several times with CH_2Cl_2, and the resulting solution was concentrated under vacuum. The complex was isolated as a yellow crystalline product (0.431 g, yield 83%) upon adding CH_3OH and cooling the solution at −20 °C. IR (Nujol): 3550 cm^{-1} (w) (ν_{O-H}). ^1H NMR (CD_2Cl_2): δ 7.42 (complex multiplet (cm), 20 H, C_6H_5), 4.50 and 4.32 (cm, 8 H, C_5H_4), −0.05 (s, broad, 1 H, OH). ^{31}P NMR: δ 6.46 (s, flanked by ^{195}Pt satellites, J = 3857 Hz). Burgundy red crystals of **4**-Pd were isolated from acetone containing 1% water, similarly to **4**-Pt. IR (Nujol): 3580 cm^{-1} (m) (ν_{O-H}). ^1H NMR (CD_2Cl_2): δ 7.7–7.3 (cm, 20 H, C_6H_5), 4.54 and 4.36 (cm, 8 H, C_5H_4), −2.32 (s, broad, 1 H, OH). ^{31}P NMR: δ 38.7 (s). Anal. Calcd for $C_{35}H_{31}BCl_2F_4FeOP_2Pd$: C, 52.09; H, 3.87. Found: C, 51.85; H, 3.85. Calcd for $C_{35}H_{31}BCl_2F_4FeOP_2Pt$: C, 44.81; H, 3.33. Found: C, 44.10; H, 3.40.

$[(dppf)Pt(DMF)_2](BF_4)_2$ (5-Pt). A solution of **1** (0.500 g, 0.609 mmol) in 5 mL of anhydrous dimethylformamide was treated with a DMF solution of $AgBF_4$ (0.238 g, 1.218 mmol). After the mixture was stirred for 30 min, the solvent was vacuum evaporated; the oily residue dissolved in CH_2Cl_2 (5 mL), and AgCl filtered off. Upon addition of toluene and cooling at −30 °C the product precipitated as mustard yellow crystals (0.33 g, 51% yield). IR (Nujol): 1640 cm^{-1} (s) (ν_{C-O}). ^1H NMR ($(CD_3)_2SO$): δ 7.96 (s, 2 H, HC(O)), 7.60 (cm, 20 H, C_6H_5), 4.64 and 4.30 (cm, 8 H, C_5H_4), 2.84 and 2.67 (s, 12 H, CH_3). ^{31}P NMR

(1) (a) Lippert, B.; Lock, C. J. L.; Rosenberg, B.; Zvagulis, M. *Inorg. Chem.* **1978**, *17*, 2971. (b) Saenger, W. *Principles of Nucleic Acid Structures*; Springer: Berlin, FRG, 1984. (c) Lippard, S. J. *Science (Washington, D.C.)* **1982**, *218*, 1075. (d) Marcelis, A. J. M.; Reedijk, J. *J. Recl. Trav. Chim. Pays-Bas* **1982**, *103*, 121. (e) Rosenberg, B. *Biochimie* **1978**, *60*, 859. (f) Schollorn, H.; Raudaschl-Sieber, G.; Muller, G.; Thewalt, U.; Lippert, B. *J. Am. Chem. Soc.* **1986**, *107*, 5932.
(2) Longato, B.; Pilloni, G.; Bonora, G. M.; Corain, B. *J. Chem. Soc., Chem. Commun.* **1986**, 1478.
(3) Furlani, A.; Scancia, V., unpublished results.
(4) Bushnel, G. W. *Can. J. Chem.* **1978**, *56*, 1773.
(5) Complex **4**-Pt was independently prepared by other authors and preliminarily communicated: Bandini, A. L.; Banditelli, G.; Minghetti, G.; Sanna, G. Proceedings of the 19th Congresso di Chimica Inorganica, Cagliari, Italy; University of Cagliari: Cagliari, Italy, 1986; Abstract A22.

† Centro di Studio sulla Stabilità e Reattività dei Composti di Coordinazione.
‡ Università di Padova.
§ Centro di Studio sui Biopolimeri.

0020-1669/88/1327-0956$01.50/0